The Application of Vector Fitting to Eigenvalue-based Harmonic Stability Analysis

Dowlatabadi, Mohammadkazem Bakhshizadeh; Yoon, Changwoo; Hjerrild, Jesper; Bak, Claus Leth; Kocewiak, ukasz Hubert; Blaabjerg, Frede; Hesselbæk, Bo

Published in:
I E E E Journal of Emerging and Selected Topics in Power Electronics

DOI (link to publication from Publisher):
10.1109/JESTPE.2017.2727503

Publication date:
2017

Document Version
Accepted author manuscript, peer reviewed version

This article has been accepted for publication in a future issue of this journal, but has not been fully edited. Content may change prior to final publication. Citation information: DOI 10.1109/JESTPE.2017.2727503, IEEE Journal of Emerging and Selected Topics in Power Electronics

The Application of Vector Fitting to Eigenvalue-based Harmonic Stability Analysis

Mohammad Kazem Bakhshizadeh, *Student Member, IEEE*, Changwoo Yoon, *Student Member, IEEE*, Jesper Hjerrild, Claus Leth Bak, *Senior Member, IEEE*, Łukasz Kocewiak, *Senior Member, IEEE*, Frede Blaabjerg, *Fellow, IEEE*, and Bo Hesselbæk

***Abstract*— Participation factor analysis is an interesting feature of the eigenvalue-based stability analysis in a power system, which enables the developers to identify the problematic elements in a multi-vendor project like in an offshore wind power plant. However, this method needs a full state space model of the elements that is not always possible to have in a competitive world due to confidentiality. In this paper, by using an identification method, the state space models for power converters are extracted from the provided data by the suppliers. Some uncertainties in the identification process are also discussed and solutions are proposed, and in the end the results are verified by time domain simulations for linear and nonlinear cases with different complexities, no matter which domain (phase or dq) is used.**

***Index Terms*— Eigenvalue analysis; Harmonic Stability; Matrix Fitting; Participation Factor Analysis; Vector Fitting**

I. Introduction

THE drastic increasing trend of global energy consumption and the demand for cleaner and more sustainable energy are bringing more new and renewable energy sources into the existing power system [1]–[3]. As a consequence of the very wide-spread renewable energy resources, the interfacing units, typically Power Electronics (PE) based power devices, are connected anywhere in the existing power system and unexpected interaction problems are caused by these newly installed PE units [4]–[7]. These interaction problems can be categorized by their frequency range into two categories. One is low-frequency small signal instability around the fundamental frequency [8]–[10] or even lower frequency, such as the sub-synchronous resonance frequency [11]–[13]. The other one is the instability with the relatively higher frequencies ranged from a few hundred Hertz to a few kilo Hertz [7], [14], [15]. Even though the physical reason of these instabilities may be different from each other, all these interaction problems can be understood by the conditions that creates unstable poles in the system transfer-function [16], [17].

There are typically two ways to assess small signal stability. One is the Impedance Based Stability Analysis (IBSA) [17] and the other one is the eigenvalue-based analysis using the State-Space (SS) model [16]. The IBSA evaluates the system's stability using the ratio of the impedance of the two sub systems (lumped impedances) that are connected to the node under study. While the eigenvalue-based method models the entire system as SS matrices, the IBSA is a simpler method but gives only local information about the stability of the system. The IBSA is confined only to an interconnection point and it needs to be remodeled repeatedly in order to assess somewhere else [18], [19]. In contrast SS models are harder to get but using them one can study the system globally. The SS model allows the participation factor analysis or the sensitivity analysis [20], [21] which is very necessary when imposing a responsibility of the interaction problem to the participants in the power network. Phenomenally, the interaction problem is a compounded issue with the linked impedances and the participant can be an offender or a victim at the same time. In that sense, it is necessary to have a quantitative method that measures the effect on the poles of the entire system (eigenvalues) from varying the state variables in each subsystem [20]. The entire SS model can be found using a systematic and modular method called Component Connection Method (CCM) [22], [23]. Also, by the help of CCM, the problematic state variables in each subsystem can be managed and visible easily [21].

However, this method is only possible on the assumption that we have proper SS models of all subsystems. The problem is with the confidentiality of the commercial products where the detailed SS model cannot be obtained and can only be reconstructed indirectly such as by Vector Fitting (VF) [24]–[26]. In [27] the application of the VF in eigenvalue-based stability analysis has been introduced, in which based on measurements from a node in the network, an SS model is proposed using the VF. However, since this model is based on a local measurement, the model is local and not global. In other words, it cannot show the dynamics of the entire system if there are some symmetries in the system, which leads to the appearance of some hidden dynamics [28], and as a result this

Manuscript received February 27, 2017; revised May 15, 2017; accepted June 27, 2016. This work was supported in part by the DONG Energy Wind Power A/S and in part by the Innovation Fund Denmark.

M. K. Bakhshizadeh, J. Hjerrild, Ł. Kocewiak, and B. Hesselbæk are with the DONG Energy Wind Power, Fredericia 7000, Denmark (e-mail: mok@et.aau.dk; jeshj@dongenergy.dk; lukko@dongenergy.dk; bohes@dongenergy.dk).

C. Yoon, C. L. Bak, and F. Blaabjerg are with the Department of Energy Technology, Aalborg University, Aalborg DK-9220, Denmark (e-mail: cyo@et.aau.dk; clb@et.aau.dk; fbl@et.aau.dk).

This article has been accepted for publication in a future issue of this journal, but has not been fully edited. Content may change prior to final publication. Citation information: DOI 10.1109/JESTPE.2017.2727503, IEEE Journal of Emerging and Selected Topics in Power Electronics

method must be repeated at different nodes. It also needs a stable system to do measurements, because if the system is unstable, then no measurement can be done and this method is not applicable. Finally, since the entire network is modelled as a black box seen from the measurement point, no further studies such as the participation factor analysis can be done to find the most problematic component in a system. It must be noted that the method proposed in this paper can be considered as an extension to [27] when more information is available.

In this paper, system stability analysis based on SS and CCM by using the indirect VF is presented. Some interaction case examples are adopted to show the validity of this procedure. The result shows that the problematic subsystem could be identified based on the participation factor analysis even for an unstable system. Since the method models the entire system using a systematic approach, it includes all dynamics of the system. Some uncertainties in the VF are also discussed.

II. Eigenvalue Analysis

A. Stability Evaluation

If one has the overall SS representation of a system, for instance as given in (1), then the stability can be evaluated by investigating the eigenvalues of matrix *A*, which is called the state (or system) matrix [29]. The eigenvalues are indeed poles of the system and if their real part is positive, then the system is unstable. It must be noted that in this paper the focus is on linear/linearized SS models.

$$\begin{aligned} \dot{x} &= Ax + Bu \\ y &= Cx + Du \end{aligned} \tag{1}$$

The eigenvalues also contain some other useful information [20], for instance if the ith eigenvalue/pole, which is called hereafter the ith mode, is

$$\lambda_i = \sigma_i + j\omega_i \tag{2}$$

Then the oscillation frequency of that mode is ω_i, the time constant of that mode, very similar to a first order RC system, is $1/\sigma_i$ and the damping is defined as

$$\xi_i = -\frac{\sigma_i}{\sqrt{\sigma_i^2 + \omega_i^2}} \tag{3}$$

In other words the transient response of the system to a perturbation includes this frequency which will decay with the specified time constant/damping. A negative damping by definition indicates an unstable case, where instead of damping, amplifying happens. Therefore, not only the stability of the system can be assessed using the sign of the real parts, but also the minimum damping of the system can be found. The latter can be considered as a measure that states how stable a system is.

B. How to find the overall SS model

One problem is how to find the SS representation of such a complicated system, which has some controllers in addition to a coupled electrical system. The Component Connection Method (CCM) is a good way to deal with very complicated systems [23]. In this method each subsystem (power converters, passive network and etc.) is modelled separately and in the end the overall SS can be found by some simple matrix operations. Modelling the system in this way is much easier and the equations are more readable. The implementation of this algorithm in a computer program is also more straightforward. In this method, first the block diagonal matrices are created by simply appending the different SS matrices individually without considering the interconnections between them.

$$\begin{aligned} \dot{x}_i &= A_i x_i + B_i u_i \\ y_i &= C_i x_i + D_i u_i \end{aligned} \tag{4}$$

$$A_{app} = \begin{bmatrix} A_1 & 0 & \dots & 0 \\ 0 & A_2 & \dots & \vdots \\ \vdots & \vdots & \ddots & 0 \\ 0 & \dots & 0 & A_n \end{bmatrix},\ x_{app} = \begin{bmatrix} x_1 \\ x_2 \\ \vdots \\ x_n \end{bmatrix} \tag{5}$$

$$B_{app} = \begin{bmatrix} B_1 & 0 & \dots & 0 \\ 0 & B_2 & \dots & \vdots \\ \vdots & \vdots & \ddots & 0 \\ 0 & \dots & 0 & B_n \end{bmatrix},\ u_{app} = \begin{bmatrix} u_1 \\ u_2 \\ \vdots \\ u_n \end{bmatrix} \tag{6}$$

$$C_{app} = \begin{bmatrix} C_1 & 0 & \dots & 0 \\ 0 & C_2 & \dots & \vdots \\ \vdots & \vdots & \ddots & 0 \\ 0 & \dots & 0 & C_n \end{bmatrix},\ y_T = \begin{bmatrix} y_1 \\ y_2 \\ \vdots \\ y_n \end{bmatrix} \tag{7}$$

$$D_{app} = \begin{bmatrix} D_1 & 0 & \dots & 0 \\ 0 & D_2 & \dots & \vdots \\ \vdots & \vdots & \ddots & 0 \\ 0 & \dots & 0 & D_n \end{bmatrix} \tag{8}$$

Then, the final matrices can be obtained by

$$\begin{aligned} u_{cmp} &= L_1 y_{cmp} + L_2 u_{sys} \\ y_{sys} &= L_3 y_{cmp} + L_4 u_{sys} \end{aligned} \tag{9}$$

where, L_1 *to* L_4 , which are called the interconnection matrices, are the matrices which define the relationship between the inputs and outputs of the individual components (u_{cmp} and y_{cmp}) and the inputs and outputs of the total system (u_{sys} and y_{sys}). The total SS model is described by

$$\begin{aligned} \dot{x}_{app} &= A_T x_{app} + B_T u_{sys} \\ y_{sys} &= C_T x_{app} + D_T u_{sys} \end{aligned} \tag{10}$$

where,

$$\begin{aligned} A_T &= A_{app} + B_{app} L_1 \left(I - D_{app} L_1\right)^{-1} C_{app} \\ B_T &= B_{app} L_1 \left(I - D_{app} L_1\right)^{-1} D_{app} L_2 + B_{app} L_2 \\ C_T &= L_3 \left(I - D_{app} L_1\right)^{-1} C_{app} \\ D_T &= L_3 \left(I - D_{app} L_1\right)^{-1} D_{app} L_2 + L_4 \end{aligned} \tag{11}$$

and *I* is the identity matrix.

C. Improper transfer functions

A transfer function is called improper, if the order of the numerator polynomial is more than the order of the denominator polynomial. The SS model of an improper transfer function could not be described by only *A*, *B*, *C* and *D*

This article has been accepted for publication in a future issue of this journal, but has not been fully edited. Content may change prior to final publication. Citation information: DOI 10.1109/JESTPE.2017.2727503, IEEE Journal of Emerging and Selected Topics in Power Electronics

matrices and another matrix E is needed to model the extra order.

$$\dot{x} = Ax + Bu$$
$$y = Cx + Du + E\dot{u} \quad (12)$$

The VF is able to find the E matrix; however, in this paper the improper transfer functions are avoided by choosing a proper impedance or admittance representation. For instance, for Current-Controlled Converters (such as solar inverters) a series inductor is normally used for smoothing the output current, therefore this series inductance makes the transfer function of the output impedance improper. However, by using the admittance model for a current controlled converter this problem can be avoided. The same can be concluded for Voltage-Controlled Converters, in which a capacitive shunt is used at the output terminal. Thus, for a Voltage-Controlled Converter an impedance model should be used. As a conclusion the E matrix is not necessary in the identification process by choosing the correct models based on the application and a little engineering judgement. If the magnitude of the frequency response goes up for higher frequencies, then it means the current model might be improper.

III. The Proposed Method for Dealing with Black Box Models

If the SS models of converters and other elements are available, then one can use the aforementioned method and evaluate the stability. However, the structure and parameters of the power converters are not always available due to confidentiality and intellectual property rights. Instead, the terminal characteristics of the converter are delivered as a look up table, which shows the frequency response of the converter to a voltage/current perturbation at a given condition. Fig. 1 shows the admittances of 5 current controlled converters [15], which are considered in this paper. It is assumed that these are the only available information. The admittances are measured in the phase domain and since the bandwidth of the Phase Locked Loop (PLL) is set too low, therefore, the coupling in the frequency response can be neglected [30], and the system can be treated as a Single Input Single Output (SISO) system [4].

In this paper, in order to find an SS model for these numerical data, the Vector Fitting (VF) is utilized. The VF is an iterative process, which tries to find a proper approximate transfer function or SS for the given frequency response [24]–[26], [31].

$$f(s) \approx \sum_{m=1}^{N} \left(\frac{R_m}{s - P_m}\right) + D + sE \quad (13)$$

where, *f(s)* is the numerical frequency response, N is the order of the transfer function, R_m is the corresponding residue of the pole P_m. D is the feed-through (direct input to output gain)

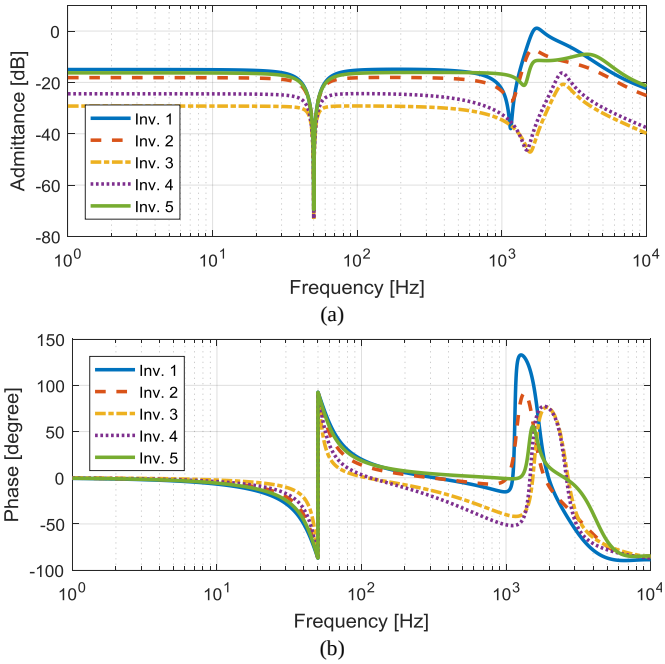

Fig. 1. The frequency characteristic of the considered converters [15] (a) the magnitude plot (b) the phase plot.

matrix and E is non-zero in cases that the transfer function is improper.

The following issues should be addressed in the approximation process: 1) up to which frequency should the fitting be done? Due to the digital nature of the controller, it is suggested to evaluate the system up to the Nyquist frequency, which is half of the sampling frequency [32], [33]. 2) What is the suggested order for the fitting process? As a general rule, the minimum order that can minimize the fitting error should be used [24]. However, there are cases where such decisions cannot be made. Therefore, in this paper an investigation is carried out with different system orders in order to see what happens if over-fitted models are used. 3) What are the effects of the measurement noise in the fitting process? In this paper for the sake of simplicity and a clearer presentation, the noise is not considered, however, there are different statistical methods to minimize the noise effect in the system identification.

IV. Simulation Results

In this section the proposed method is explained by two test cases. The first case is formed of 5 converters and is a simple study case where all models are linear. The second case is a more comprehensive case, which includes an active inverter and an active rectifier, and the effects of the Signal Conditioning Filter (SCF), PLL and dc link voltage controller are considered. In the first case, since the model is linear and symmetrical, the study is carried out in the phase domain. However, for the second case the linearization is performed in the synchronous reference frame.

This article has been accepted for publication in a future issue of this journal, but has not been fully edited. Content may change prior to final publication. Citation information: DOI 10.1109/JESTPE.2017.2727503, IEEE Journal of Emerging and Selected Topics in Power Electronics

A. A Linear Case study

Fig. 2 shows the considered power system, which is based on to the Cigré LV benchmark system [34]. The current control is done using a Proportional Resonant controller as shown in Fig. 2, and the parameters of the electrical system and controllers are listed in Table I. Depending on which converters are connected or disconnected, different stable and unstable cases can be seen [15], [35]. Table II shows a few different configurations and Fig. 3 is the time domain simulation considering those cases.

Fig. 4 shows the magnitude plot of the admittance of Inverter 2 and the accuracy of the identified models (magnitude of the absolute error) with 6th, 8th and 12th orders by the VF. It must be noted that since the original admittance plots are results of a measurement, therefore, they must model a stable system. To ensure that no Right Half Plane (RHP) pole appears in the identified models, the stability enforcement must be used, which simply rejects unstable poles in each iteration. For elements where the transfer function is accessible, one can find the equivalent SS representation. For instance, the SS equations of the network can directly be obtained from the differential equations describing the system dynamics (notice the notations and directions in Fig. 2) as (14) and (15).

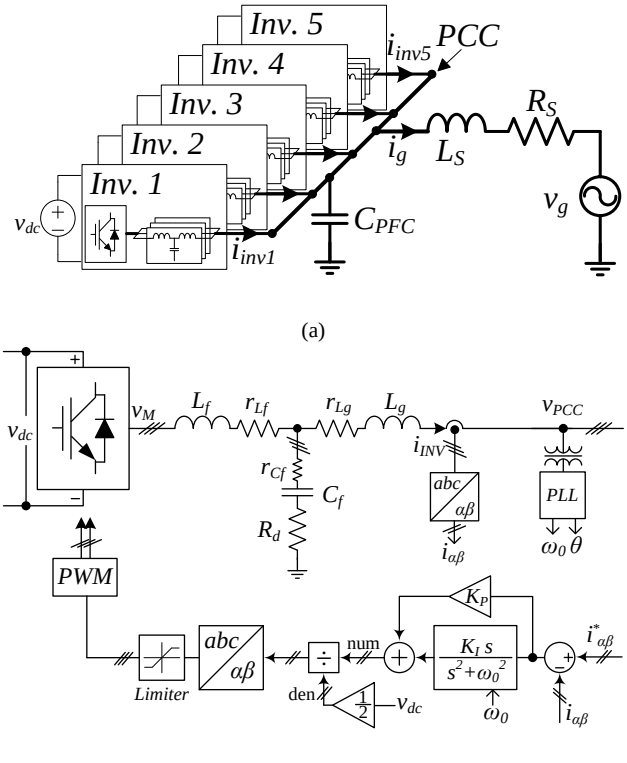

Fig. 2. The considered power system [15], which is based on Cigré LV benchmark system [34]: a) the overall power scheme. (b) the converter internal control structure.

TABLE I. THE PARAMETERS OF THE CONSIDERED POWER SYSTEM [15].

Symbol / Description		Inverters				
		1	2	3	4	5
f_{sw}	Switching/Sampling frequency [kHz]	10		16		10
V_{dc}	DC-link voltage [V]	750				
L_f	Inverter side inductor of the filter [mH]	0.87	1.2	5.1	3.8	0.8
C_f	Filter capacitor [μF]	22	15	2	3	15
L_g	Grid side inductor of the filter [mH]	0.22	0.3	1.7	1.3	0.2
r_{Lf}	Parasitic resistance of L_f [mΩ]	11.4	15.7	66.8	49.7	10
r_{Cf}	Parasitic resistance of C_f [mΩ]	7.5	11	21.5	14.5	11
r_{Lg}	Parasitic resistance of L_g [mΩ]	2.9	3.9	22.3	17	2.5
R_d	Damping resistance [Ω]	0.2	1.4	7	4.2	0.9
K_p	Proportional gain of the controller	5.6	8.05	28.8	16.6	6.5
K_i	Integrator gain of the controller	1000		1500		1000
L_s	Grid inductance [mH]	0.4				
R_s	Grid resistance [Ω]	0.1				

TABLE II. DIFFERENT CONFIGURATIONS OF 0AND THE CORRESPONDING RESULTS [15]

Case No.	Description	Result
1	All are connected	Stable
2	Inverter 5 is disconnected	Unstable
3	Inverter 2 is disconnected	Unstable
4	Inverter 3 is disconnected	Stable
5	Inverter 3 and 4 are disconnected	Stable

Fig. 5 shows the considered power system as a control block diagram in order to show how CCM can be utilized. The L_1, L_2, L_3 and L_4 interconnection matrices of (9) and (11) are given as (16). The inputs and outputs are highlighted with red and blue signals, respectively. The elements of u_{cmp} and y_{cmp}

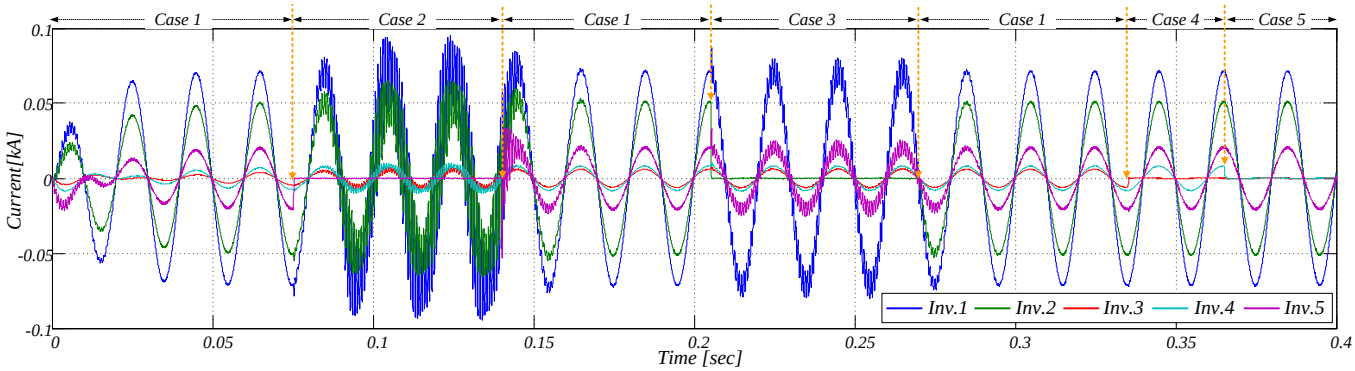

Fig. 3. Time domain simulations for different cases [15] shown in Table II.

This article has been accepted for publication in a future issue of this journal, but has not been fully edited. Content may change prior to final publication. Citation information: DOI 10.1109/JESTPE.2017.2727503, IEEE Journal of Emerging and Selected Topics in Power Electronics

vectors are also highlighted in the Fig. 5. Any signal can be considered as the system input and output, however as an example, the grid voltage v_g is considered as the input to the overall system and v_{pcc} is considered as the output.

$$L_1 = \begin{bmatrix} [0]_{5\times5} & [1]_{5\times1} \\ 0 & 0 \\ [I]_{5\times5} & [0]_{5\times1} \end{bmatrix}, L_2 = \begin{bmatrix} [1]_{5\times1} \\ [0]_{6\times1} \end{bmatrix} \quad (16)$$

$$L_3 = [[0]_{1\times5} \quad 1], L_4 = [0]$$

1) Challenges in the VF

The CCM as described above can be utilized to build up the entire SS model of the system and to study the system dynamics [23]. Fig. 6 shows the pole plot of the entire system (for Case 5) for different identification orders that is zoomed in for a better view and the reader cannot see all the high frequency poles. Time domain simulations for a detailed switching model as shown in Fig. 3 indicate the stable operation of Case 5. However, there are some RHP poles in the identified system as listed in Table III.

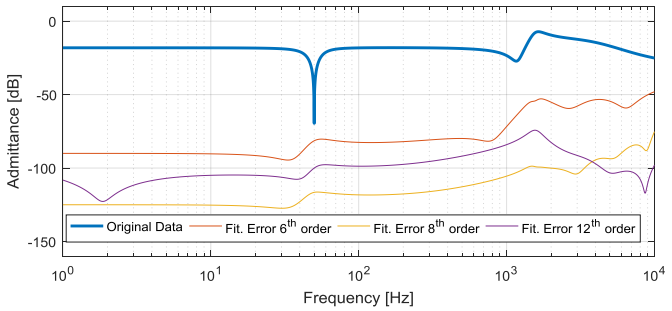

Fig. 4. The original data (admittance of Inverter 2) and the fitting errors for different fitting orders.

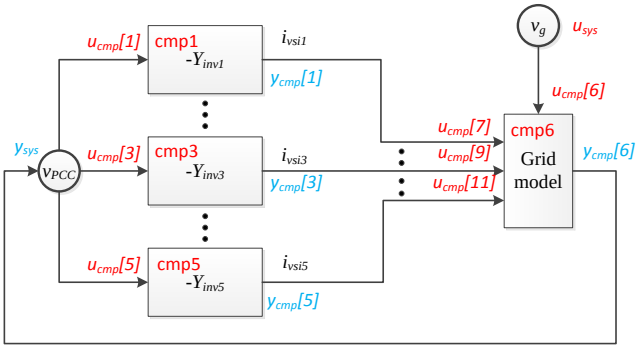

Fig. 5. The considered power system in Fig. 2 as a control block diagram.

$$C_{PFC}\frac{a}{dt}v_{pcc} + i_g = i_{inv1} + i_{inv2} + i_{inv3} + i_{inv4} + i_{inv5} \quad (14)$$

$$v_{pcc} = L_s\frac{d}{dt}i_g + R_s i_g + v_g$$

$$\dot{x} = A_{net}x + B_{net}u = \begin{bmatrix} -\frac{R_s}{L_s} & \frac{1}{L_s} \\ \frac{-1}{C_{PFC}} & 0 \end{bmatrix}\begin{bmatrix} i_g \\ v_{pcc} \end{bmatrix} + \begin{bmatrix} -\frac{1}{L_s} & 0 & 0 & 0 & 0 & 0 \\ 0 & \frac{1}{C_{PFC}} & \frac{1}{C_{PFC}} & \frac{1}{C_{PFC}} & \frac{1}{C_{PFC}} & \frac{1}{C_{PFC}} \end{bmatrix}\begin{bmatrix} v_g \\ i_{inv1} \\ i_{inv2} \\ i_{inv3} \\ i_{inv4} \\ i_{inv5} \end{bmatrix} \quad (15)$$

$$y = [v_{pcc}] = C_{net}x + D_{net}u = [0 \quad 1]x + [0 \quad 0 \quad 0 \quad 0 \quad 0 \quad 0]u$$

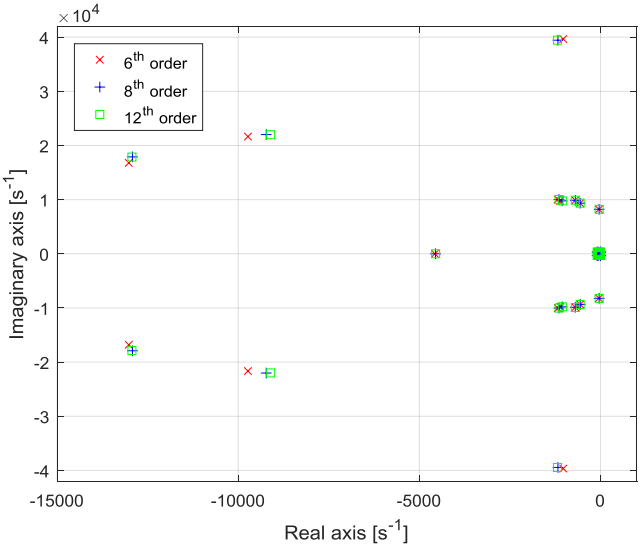

Fig. 6. The pole plot of the entire system (as shown in Fig. 2) for Case 5.

TABLE III. THE UNSTABLE POLES OF THE SYSTEM SHOWN IN 0

Unstable poles depending on the order [s^{-1}]		
6^{th}	8^{th}	12^{th}
-	1.04e7	1.69e6
-	0.88e7	4.46e4±j1.56e5

One may think that the unstable identified poles are caused by overfitting, because the unstable poles do not appear for the 6^{th} order, but the problem is indeed caused by the lack of information for the frequencies beyond the trained range of the frequency. Fig. 7 shows the sum of admittances of the converters for Case 5 (Y_1+Y_2+Y_5) for the original data and the fitted data with different orders. It can be seen that at the high frequency range, beyond the trained range, there is a non-passive region, which causes those unstable poles reported in TABLE III for the 8^{th} order model. Actually, this is the reason why passivity enforcement is necessary in the VF. Passivity enforcement is the process during the VF to make sure that the model is passive at all frequencies even beyond the trained range [36]. This can be done by enforcing the Hamiltonian matrix of the identified system to have no imaginary eigenvalues [37]. Passivity enforcement is necessary in approximating the passive elements such as transformers, because the models will afterwards be used in time domain simulations and if they are non-passive, they might make the system unstable. However, this is not a

This article has been accepted for publication in a future issue of this journal, but has not been fully edited. Content may change prior to final publication. Citation information: DOI 10.1109/JESTPE.2017.2727503, IEEE Journal of Emerging and Selected Topics in Power Electronics

concern in this study, because: 1) the aim of this paper is not to develop a model for time domain simulations, in fact evaluating the stability is the target here. 2) a power converter is not a passive component due to [33]: a) the time delay, computational and PWM delay which affect the high frequency region b) The current controller which affects the current control bandwidth (for example a Constant Power Load introduces a negative resistance in the control bandwidth) c) The low frequency outer loop controllers (e.g. PLL, voltage and power controller), which affect the low frequency range.

Therefore, the passivity enforcement is not applicable for power converter approximation. The proposed workaround in this paper is to limit the frequency of the identified poles of the total system. In other words the system is trained up to 10 kHz, therefore, the identified poles beyond this range must be disregarded. It can easily be done by removing the poles, which are outside the confidence circle as shown in Fig. 8.

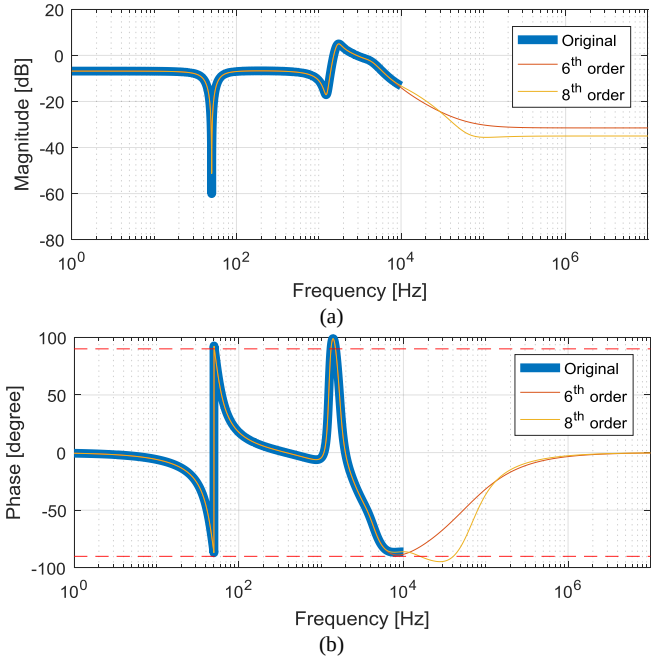

Fig. 7. The bode plot of the aggregated admittance of converters for the original data and the approximated models for Case 5. (a) magnitude plot (b) phase plot.

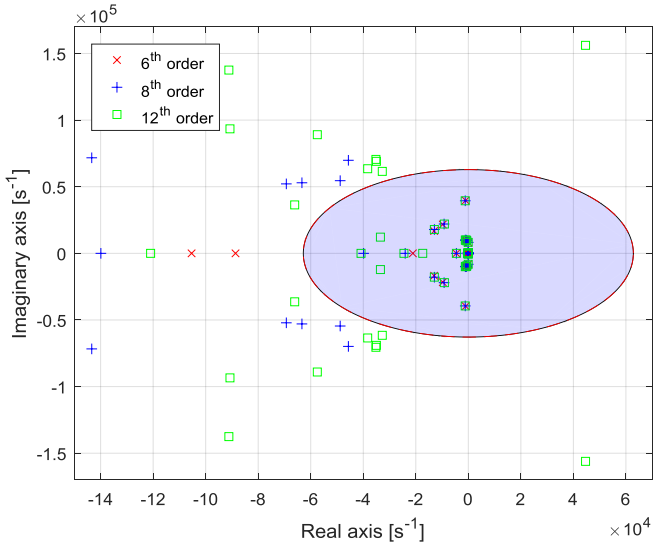

Fig. 8. The poles outside of the confidence circle must be disregarded (this is for Case 5).

2) Participation factor analysis

By removing the high frequency poles from the study, the Participation Factor (PF) analysis can be done by some simple matrix operations [20], [21]. For the ith pole, the participation analysis can be done using

$$P_{ki} = \frac{\partial \lambda_i}{\partial a_{kk}} = \Phi_{ki}\Psi_{ik} \tag{17}$$

where, Φ_i is the right eigenvector of the i^{th} eigenvalue, Ψ_i is the left eigenvector of the i^{th} eigenvalue, and P_{ki} indicates the contribution of the k^{th} state on the i^{th} pole.

In this section Case 2, which is unstable, is considered [15], [35]. It can be seen in Fig. 9 that the instability is due to an eigenvalue at (229±j8180) rad/s. Table IV shows the five largest contributors to this unstable pole and also indicates that despite different approximation orders they identify the contribution levels to be almost the same. It can be seen that Inverter 1 has the most contribution to the unstable pole. Since the model is a black box, no more conclusions can be made on which part of Inverter 1 is causing the instability. However, by informing the supplier about this, they can improve the stability by looking at the frequency of stability.

3) Time domain simulations

As discussed in section II.A, an eigenvalue contains information about the transient response, i.e. how fast the transient decays/grows and at which frequency. In this section,

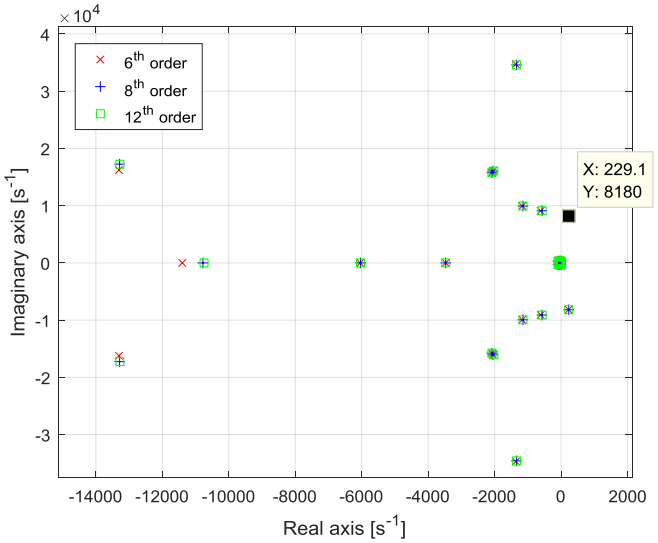

Fig. 9. Pole plot of Case 2, where an unstable pole is highlighted.

TABLE IV. THE PARTICPATION FACTOR ANALYSIS FOR CASE 2 THAT IS UNSTABLE.

6th order		8th order		12th order	
State Name	PF	State Name	PF	State Name	PF
INV1.State 3	0.296	INV1.State 4	0.294	INV1.State 5	0.295
INV1.State 4	0.302	INV1.State 5	0.300	INV1.State 6	0.300
INV2.State 3	0.167	INV2.State 3	0.167	INV2.State 7	0.167
INV2.State 4	0.169	INV2.State 4	0.169	INV2.State 7	0.169
Grid.State 1	0.112	Grid.State 1	0.112	Grid.State 1	0.112

This article has been accepted for publication in a future issue of this journal, but has not been fully edited. Content may change prior to final publication. Citation information: DOI 10.1109/JESTPE.2017.2727503, IEEE Journal of Emerging and Selected Topics in Power Electronics

the previously presented cases are reviewed again by means of time domain simulations. Simulations are carried out in PLECS [38] using a very detailed switching model. The controller is exactly modeled by using triggered subsystems to mimic the sampled-based control loop in a real DSP. The single update PWM is used in this paper, which is the reason the sampling and switching frequencies are equal. The most critical eigenvalue, which has the lowest damping, in Case 5 is -64 ± 8254j, which indicates an oscillation frequency of 8254 rad/s and a time constant of -1/64 seconds. It can be seen in Fig. 10 that the oscillation frequency in Case 5 after a perturbation is accurately anticipated. The measured time constant is also roughly correct, since the oscillation magnitude (peak to peak) is changed -61 % from t_1=0.201 to t_2=0.211 [s]. However, a -47% drop is predicted by the decaying/growing exponential function (18).

$$\frac{I_2}{I_1} = e^{(t_2 - t_1)/\tau} \tag{18}$$

where, $\tau=1/\sigma$ is the time constant (for a stable pole it is negative), and I_2 and I_1 are the current magnitudes at $t=t_2$ and $t=t_1$, respectively.

Similar study is also done for the Case 2, which is unstable. The unstable eigenvalues are 229±j8180 rad/s. The highlighted oscillation frequency in Fig. 11 is almost the same the imaginary part of the predicted eigenvalue. In the simulation the peak to peak magnitude is changed 962% from t_1=0.203 to t_2=0.213 [s], which indicates a good correlation with the predicted change of 887% using (18).

B. A nonlinear case

Linearized models should be used for small-signal stability analysis of nonlinear systems. Therefore, the first step in analyzing the stability using the proposed method is to find the steady state operating point that can be obtained after a load flow. In this paper the linearization is performed in a synchronously rotating frame (the dq frame), where each ac quantity can be modelled by two dc signals (d- and q-channels).

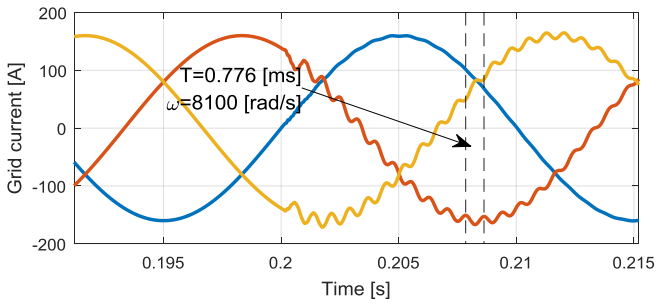

Fig. 10. Time domain results for Case 5, where the system remains stable after a perturbation.

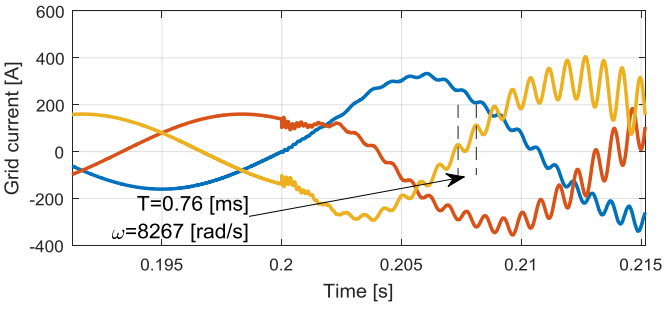

Fig. 11. Time domain results for Case 2, where the system loses stability after a perturbation.

In contrast to linear systems, the linearized nonlinear models are dependent on an operating point, and as shown in [39], by changing the operating point the admittance/impedance characteristics would be different. Therefore, for each condition (e.g. different active and reactive power generation) a new set of numerical data should be used for identification. In [39] it has been shown that by some simple sensitivity studies the admittance/impedance can be found for any operating point. It should also be noted that power system elements are mostly operated very close to the nominal conditions. Therefore, assuming a constant admittance profile for studies seems reasonable. Furthermore, it should also be taken into account that providing the correct data for studies is the suppliers' responsibility. Therefore, in this part the given characteristics are for the given operating point and finding the operating point dependent characteristics is out of scope of this paper.

Another important point is that the nonlinear behavior in the power electronic devices mostly happens in the low frequency range (i.e. less than two times the fundamental frequency) due to the fact that the outer loop controllers have a bandwidth much slower than the current controller. Therefore, if the objective is to study the interactions in the harmonic frequency range (medium to high frequency), linear models can be used in a similar way to the previous case, where PLL dynamics are neglected [4].

Outer loop control (dc link control, power control and synchronization loop) generally results in an Multi-Input Multi-Output (MIMO) control system, where the impedance characteristics cannot be considered as in a SISO system [30], [40]. In phase (sequence) domain modelling, they result in appearance of some frequency couplings, i.e. if a small signal voltage perturbation is applied at the converter terminals, then the converter will respond with different frequencies. In the case of a balanced system with a current controller in the dq frame and a simple SRF PLL, the response includes ω_p and ω_p-$2\omega_1$ where ω_p is the perturbation frequency and ω_1 is the fundamental frequency. Then a 2x2 matrix must be used as the converter admittance/impedance for small signal stability analysis. In the dq domain modelling, normally impedances are defined as 2x2 dq impedances, and since the operating point is a dc signal (as long as the system is balanced) in the dq frame the aforementioned frequency couplings do not happen.

In this section to study the effects of the synchronization loop (PLL) and the dc link control, a test case as shown in Fig. 12 is considered. The Voltage Source Inverter (VSI) injects active current to the PCC while the Active Front End (AFE) feeds a dc load by absorbing active power from the PCC. This system is based on the test system considered in [41] and the parameters are listed in Table V. The power circuit and the

This article has been accepted for publication in a future issue of this journal, but has not been fully edited. Content may change prior to final publication. Citation information: DOI 10.1109/JESTPE.2017.2727503, IEEE Journal of Emerging and Selected Topics in Power Electronics

control structure of the VSI and the AFE are shown in Fig. 13. The SCF block acts as a low-pass filter to attenuate the high frequency content from the measurements. The dc link in the AFE is controlled by a PI controller, which absorbs more active power if there is a drop in dc link voltage. The terminal characteristics as shown in Fig. 14 are obtained from the equations developed in [41] for admittance modelling of converters in the dq domain for this specific operating point (the impedance can also be measured in the dq domain), and finally the same methodology as in the previous case is followed here. The admittances are not SISO, hence, the Matrix Fitting (MF) should be utilized, which is the MIMO version of the VF [24]–[26], [31]. It must be noted that a slightly different method than [31] should be used because [31] assumes the transfer function matrix is symmetrical, which is not the case in dq impedances.

Two scenarios are reported in this part, one is stable and the other one is intentionally made unstable by increasing the integrator gain of the PLL of the VSI (see Table V). Fig. 14 shows the original admittance data where the difference is located at the low frequency range, since the PLL is changed. The SS model of the network can be obtained as

$$\dot{x} = A_{net}x + B_{net}u = \begin{bmatrix} -\frac{R_g}{L_g} & -\frac{1}{L_g} \\ \frac{1}{C_L} & -\frac{1}{C_L R_L} \end{bmatrix}\begin{bmatrix}\Delta i_g \\ \Delta v_x\end{bmatrix} + \begin{bmatrix} \frac{1}{L_g} & 0 & 0 \\ 0 & \frac{1}{C_L} & \frac{1}{C_L} \end{bmatrix}\begin{bmatrix}\Delta v_g \\ \Delta i_1 \\ \Delta i_2\end{bmatrix} \quad (19)$$

$$y = \begin{bmatrix}\Delta i_g \\ \Delta v_x\end{bmatrix} = C_{net}x + D_{net}u = \begin{bmatrix}1 & 0 \\ 0 & 1\end{bmatrix}x + \begin{bmatrix}0 & 0 & 0 \\ 0 & 0 & 0\end{bmatrix}u$$

where, Δ is used to emphasize that small signal incremental equations are used. It should be noted that the above equations are valid for a single-phase system. For a three-phase system

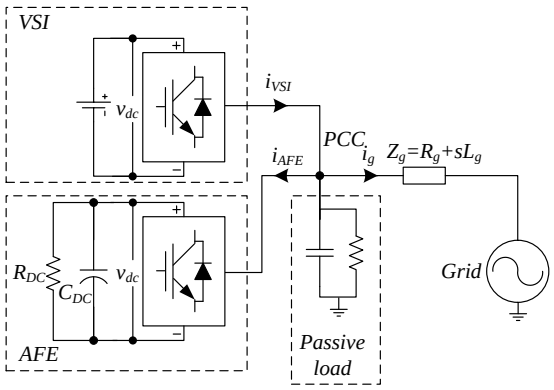

Fig. 12. The considered nonlinear power system [41] with a Voltage Source Inverter (VSI) and an Active Front End (AFE).

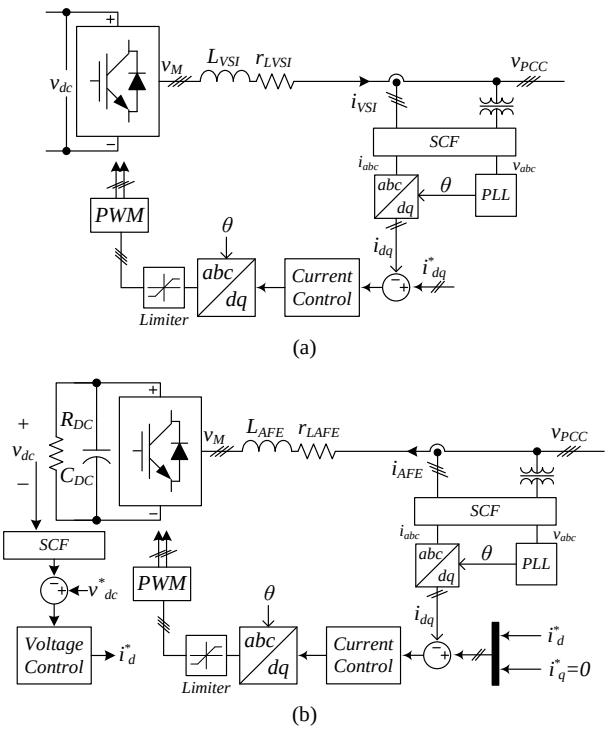

Fig. 13. The power circuit and control structure of (a) the Voltage Source Inverter (b) the Active Front End.

TABLE V. PARAMETERS OF THE NONLINEAR POWER SYSTEM.

Symbol	Description	Value
System Parameters		
V_g	Grid voltage (phase voltage rms) [V]	120
f_g	Grid frequency [Hz]	60
R_L	Resistance of local passive load [Ω]	10
C_L	Capacitance of local passive load [μF]	250
L_g	Grid inductance [mH]	0.2
R_g	Grid resistance [Ω]	1.1
Parameters of the VSI		
L_{VSI}	Inductance of the inverter [mH]	1.0
r_{LVSI}	Self-resistance of L_{VSI} [mΩ]	120
V_{dc}	DC link voltage [V]	600
$i^*_{d\text{-}vsi}$	d channel current reference [A]	140
$i^*_{q\text{-}vsi}$	q channel current reference [A]	0
k_{piVSI}	Proportional gain of current controller	0.0105
k_{iiVSI}	Integrator gain of current controller	1.1519
$k_{ppllVSI}$	Proportional gain of PLL	0.1
$k_{ipllVSI}$	Integrator gain of PLL	0.32 (stable) 5.2 (unstable)
Parameters of the AFE		
L_{AFE}	Inductance of the AFE [mH]	0.5
r_{LAFE}	Self-resistance of L_{AFE} [mΩ]	90
C_{dcAFE}	Dc link capacitor [μF]	100
R_{dc}	Dc load resistance [Ω]	13.825
V^*_{dc}	DC link voltage reference [V]	600
$i^*_{q\text{-}vsi}$	q channel current reference [A]	0
k_{piAFE}	Proportional gain of current controller	0.0052
k_{iiAFE}	Integrator gain of current controller	1.152
k_{pvAFE}	Proportional gain of dc link voltage controller	0.0628
k_{ivAFE}	Integrator gain of dc link voltage controller	45.45
$k_{ppllVSI}$	Proportional gain of PLL	0.05
$k_{ipllVSI}$	Integrator gain of PLL	0.5
Common Parameters		
SCF	Signal Conditioning Filter	$\frac{\omega_n^2}{s^2 + 2\xi\omega_n + \omega_n^2}$
ω_n	Natural frequency of SCF [rad/s]	1.23e6
ξ	Damping factor of SCF [rad/s]	4.74e-13
f_{sw}	Switching/sampling frequency [kHz]	20
T_{del}	Time delay due to the digital control and PWM	$1.5/f_{sw}$

This article has been accepted for publication in a future issue of this journal, but has not been fully edited. Content may change prior to final publication. Citation information: DOI 10.1109/JESTPE.2017.2727503, IEEE Journal of Emerging and Selected Topics in Power Electronics

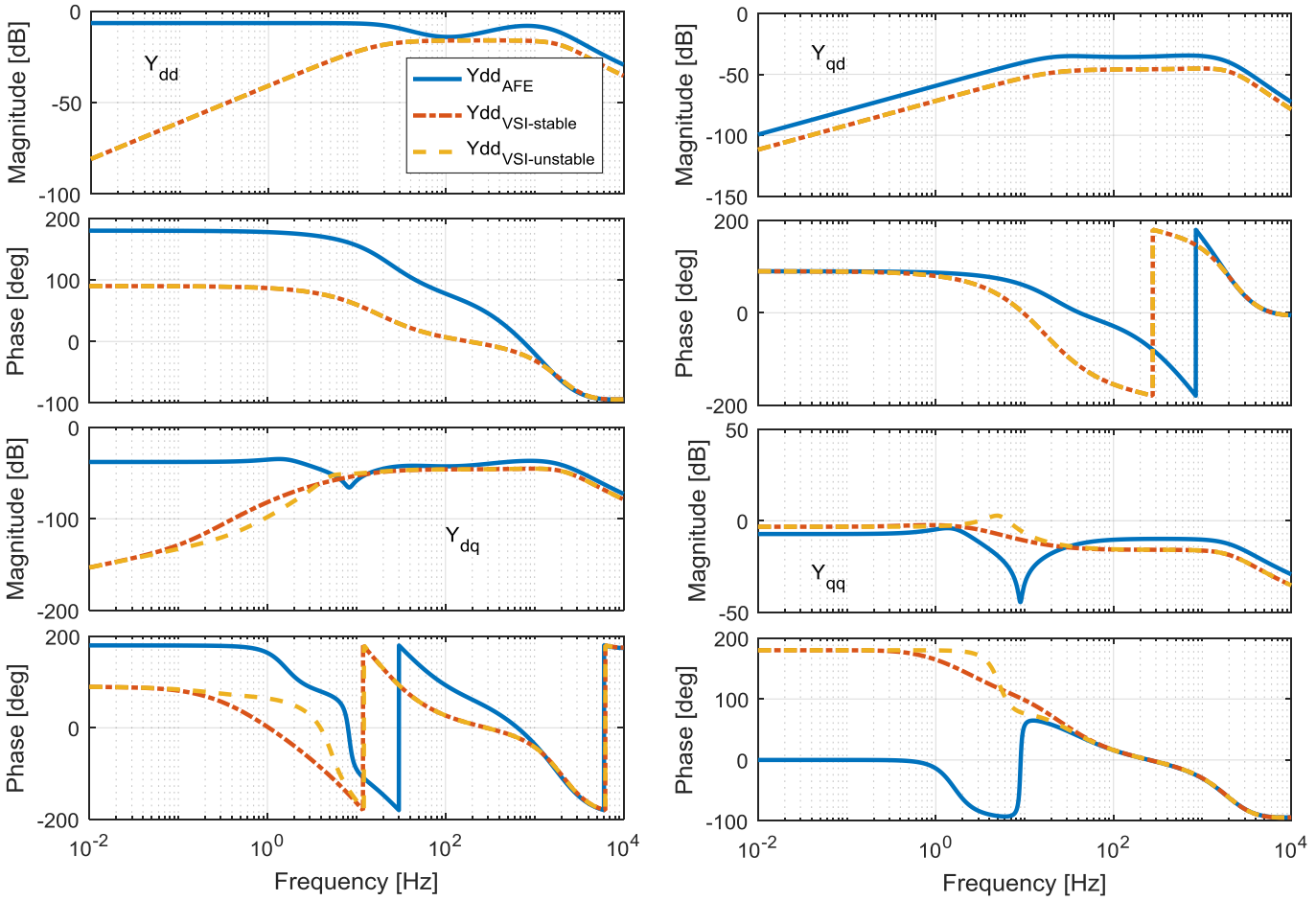

Fig. 14. The admittances of the AFE and the VSI for stable and unstable designs in dq domain.

the equations can be transformed into dq domain [42] using

$$A_{dq}=\begin{bmatrix}A_{net} & -\omega_1 I\\ \omega_1 I & A_{net}\end{bmatrix}, B_{dq}=\begin{bmatrix}B_{net} & 0\\ 0 & B_{net}\end{bmatrix},$$
$$C_{dq}=\begin{bmatrix}C_{net} & 0\\ 0 & C_{net}\end{bmatrix}, D_{dq}=\begin{bmatrix}D_{net} & 0\\ 0 & D_{net}\end{bmatrix} \quad (20)$$

where, I is the identity matrix of the appropriate size.

Now the CCM can be applied to get the overall SS matrices of the whole system. Fig. 15 shows the identified poles of the system for the stable (in blue) and unstable (in red) cases. Fig. 16 shows the time domain results of the PLL output of the VSI

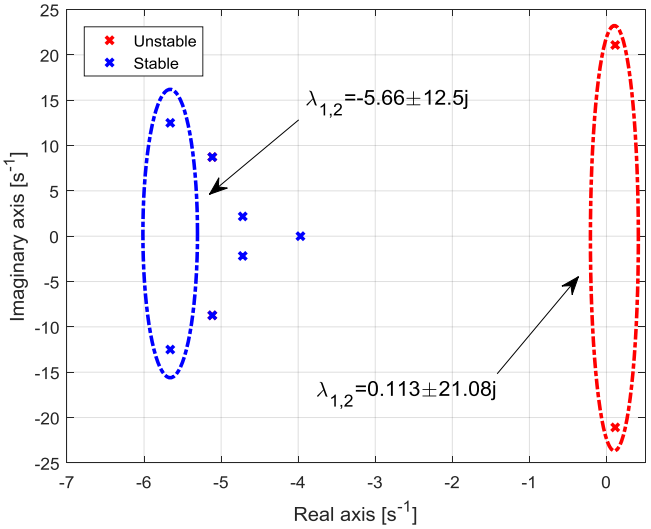

Fig. 15. The eigenvalues of the entire system for stable and unstable cases (notice only low frequency poles are shown).

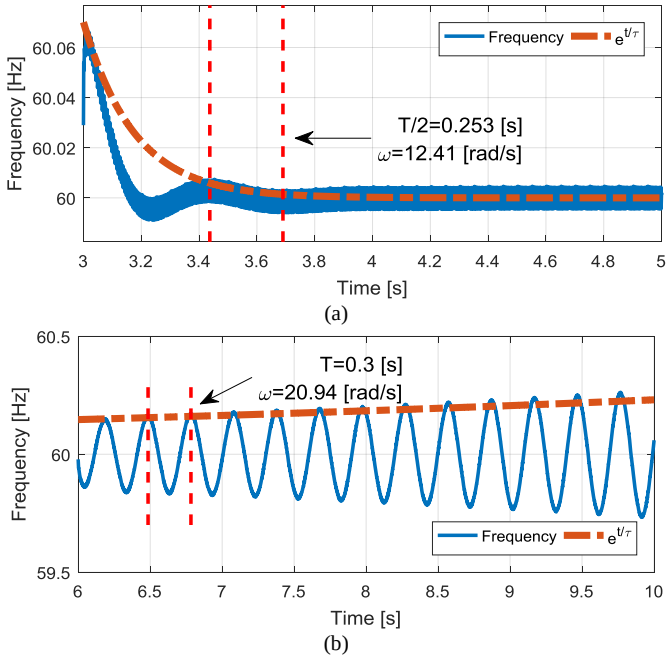

Fig. 16. Time domain simulations of the nonlinear system for (a) stable case (b) the unstable case. The damping and oscillation frequency are highlighted.

for stable and unstable cases when a perturbation is applied. The measured frequencies in Fig. 16 are almost the same as the imaginary part of the highlighted poles, which are the poles with the minimum damping. Furthermore, the exponential curves in Fig. 16 (a) and (b), which are based on the real part of the predicted poles as mentioned in (18), show a good agreement between the time constant in the simulations with the proposed method.

1) Participation Factor Analysis

By using (17) the participation factor analysis for the unstable pole in the second case is carried out. Table VI shows the three largest contributors to this instability, where it meets the expectation, since the reason of instability was the increase in the PLL gain of the VSI.

TABLE VI. THE PARTICPATION FACTOR ANALYSIS FOR THE UNSTABLE CASE.

State Name	PF
VSI.State 15	0.44
VSI.State 16	0.35
AFE.State 17	0.19

V. CONCLUSION

In this paper, the eigenvalue-based stability analysis is used to evaluate stability of a system with multiple converters. The converters are modelled as black boxes where no information about the internal structure and parameters are available. The VF is used to find a proper SS model, however there are uncertainties in the modelling. It is shown that some models might result in a non-passive model and a method is proposed to exclude the irrelevant poles from the study. Also, the participation factor analysis is utilized to quantify how much each component is responsible for the observed instability. A nonlinear case with synchronization loops and a dc link voltage control, which is linearized in the dq domain, is also presented to show that the Matrix Fitting can successfully be used for the analysis of MIMO systems.

REFERENCES

[1] F. Blaabjerg, Z. Chen, and S. B. Kjaer, "Power Electronics as Efficient Interface in Dispersed Power Generation Systems," *IEEE Trans. Power Electron.*, vol. 19, no. 5, pp. 1184–1194, Sep. 2004.

[2] "EU 2030 Energy strategy,"[online]. Available: http://ec.europa.eu/energy/en/topics/energy-strategy/2030-energy-strategy

[3] Frankfurt School-UNEP Centre/BNEF. 2016., "Global Trends In Renewable Energy Investment 2016," [online]. Available: http://www.fs-unep-centre.org

[4] X. Wang, F. Blaabjerg, and W. Wu, "Modeling and Analysis of Harmonic Stability in an AC Power-Electronics-Based Power System," *IEEE Trans. Power Electron.*, vol. 29, no. 12, pp. 6421–6432, 2014.

[5] L. Harnefors, A. G. Yepes, A. Vidal, and J. Doval-Gandoy, "Passivity-Based Controller Design of Grid-Connected VSCs for Prevention of Electrical Resonance Instability," *IEEE Trans. Ind. Electron.*, vol. 62, no. 2, pp. 702–710, 2015.

[6] E. Möllerstedt and B. Bernhardsson, "Out of control because of harmonics. An analysis of the harmonic response of an inverter locomotive," *IEEE Control Syst. Mag.*, vol. 20, no. 4, pp. 70–81, 2000.

[7] J. H. R. Enslin and P. J. M. Heskes, "Harmonic Interaction Between a Large Number of Distributed Power Inverters and the Distribution Network," *IEEE Trans. Power Electron.*, vol. 19, no. 6, pp. 1586–1593, Nov. 2004.

[8] L. Harnefors, M. Bongiorno, and S. Lundberg, "Input-Admittance Calculation and Shaping for Controlled Voltage-Source Converters," *IEEE Trans. Ind. Electron.*, vol. 54, no. 6, pp. 3323–3334, Dec. 2007.

[9] B. Wen, D. Boroyevich, P. Mattavelli, Z. Shen, and R. Burgos, "Influence of Phase-Locked Loop on dq Frame Impedance of Three-Phase Voltage-Source Converters and the Impact on System Stability," in *2013 CPES Power Electron. Conf.*, pp. 1–11, 2013.

[10] F. Demello and C. Concordia, "Concepts of Synchronous Machine Stability as Affected by Excitation Control," *IEEE Trans. Power Appar. Syst.*, vol. PAS-88, no. 4, pp. 316–329, Apr. 1969.

[11] M. Cespedes, L. Xing, and J. Sun, "Constant-Power Load System Stabilization by Passive Damping," *IEEE Trans. Power Electron.*, vol. 26, no. 7, pp. 1832–1836, Jul. 2011.

[12] N. Pogaku, M. Prodanovic, and T. C. Green, "Modeling, Analysis and Testing of Autonomous Operation of an Inverter-Based Microgrid," *IEEE Trans. Power Electron.*, vol. 22, no. 2, pp. 613–625, Mar. 2007.

[13] N. Bottrell, M. Prodanovic, and T. C. Green, "Dynamic Stability of a Microgrid With an Active Load," *IEEE Trans. Power Electron.*, vol. 28, no. 11, pp. 5107–5119, Nov. 2013.

[14] J. Sun, "Impedance-based stability criterion for grid-connected inverters," *IEEE Trans. Power Electron.*, vol. 26, no. 11, pp. 3075–3078, 2011.

[15] C. Yoon, H. Bai, R. N. Beres, X. Wang, C. L. Bak, and F. Blaabjerg, "Harmonic Stability Assessment for Multiparalleled, Grid-Connected Inverters," *IEEE Trans. Sustain. Energy*, vol. 7, no. 4, pp. 1388–1397, Oct. 2016.

[16] P. Kundur, N. J. Balu, and M. G. Lauby, *Power system stability and control*. McGraw-Hill, 1994.

[17] R. D. Middlebrook, "Input filter considerations in design and application of switching regulators," in *Proc. IEEE Ind. Appl. Soc.Annu. Meeting*, 1976, pp. 91–107.

[18] C. Yoon, H. Bai, X. Wang, C. L. Bak, and F. Blaabjerg, "Regional modeling approach for analyzing harmonic stability in radial power electronics based power system," in *2015 IEEE 6th International Symposium on Power Electronics for Distributed Generation Systems (PEDG)*, 2015, pp. 1–5.

[19] C. Yoon, X. Wang, C. Leth Bak, and F. Blaabjerg, "Stabilization of Multiple Unstable Modes for Small- Scale Inverter-Based Power Systems with Impedance- Based Stability Analysis," in *2015 IEEE Applied Power Electronics Conference and Exposition - APEC 2015*, pp. 1202-1208, 2015.

[20] P. Kundur, *Power System Stability and Control*. McGraw-Hill, 1994.

[21] Y. Wang, X. Wang, F. Blaabjerg, and Z. Chen, "Harmonic Instability Assessment Using State-Space Modeling and Participation Analysis in Inverter-Fed Power Systems," *IEEE Trans. Ind. Electron.*, pp. 806-816, 2016.

[22] G. Gaba, S. Lefebvre, and D. Mukhedkar, "Comparative analysis and study of the dynamic stability of AC/DC systems," *IEEE Trans. Power Syst.*, vol. 3, no. 3, pp. 978–985, Aug. 1988.

[23] Y. Wang, X. Wang, F. Blaabjerg, and Z. Chen, "Harmonic stability analysis of inverter-fed power systems using Component Connection Method," in *2016 IEEE 8th International Power Electronics and Motion Control Conference (IPEMC-ECCE Asia)*, 2016, pp. 2667–2674.

[24] B. Gustavsen and A. Semlyen, "Rational approximation of frequency domain responses by vector fitting," *IEEE Trans. Power Deliv.*, vol. 14, no. 3, pp. 1052–1061, Jul. 1999.

[25] B. Gustavsen, "Improving the Pole Relocating Properties of Vector Fitting," *IEEE Trans. Power Deliv.*, vol. 21, no. 3, pp. 1587–1592, Jul. 2006.

[26] D. Deschrijver, M. Mrozowski, T. Dhaene, and D. De Zutter, "Macromodeling of Multiport Systems Using a Fast Implementation of the Vector Fitting Method," *IEEE Microw. Wirel. Components Lett.*, vol. 18, no. 6, pp. 383–385, Jun. 2008.

[27] A. Rygg, M. Amin, M. Molinas, and B. Gustavsen, "Apparent impedance analysis: A new method for power system stability analysis," in *2016 IEEE 17th Workshop on Control and Modeling for Power Electronics (COMPEL)*, pp. 1–7, 2016.

[28] J. L. Agorreta and M. Borrega, "Modeling and Control of N -Paralleled

Grid- Connected Inverters With LCL Filter Coupled Due to Grid Impedance in PV Plants," *IEEE Trans. Power. Electron.*, vol. 26, no. 3, pp. 770–785, 2011.

[29] K. Ogata, *Modern control engineering*. Prentice Hall, 2002.

[30] M. K. Bakhshizadeh, X. Wang, F. Blaabjerg, J. Hjerrild, L. Kocewiak, C. L. Bak, and B. Hesselbek, "Couplings in Phase Domain Impedance Modelling of Grid-Connected Converters," *IEEE Trans. Power Electron.*, vol. 31, no. 10, pp. 6792–6796, 2016.

[31] "The Vector Fitting Web Site." [Online]. Available: https://www.sintef.no/projectweb/vectfit/.

[32] L. Harnefors, L. Zhang, and M. Bongiorno, "Frequency-domain passivity-based current controller design," *IET Power Electron.*, vol. 1, no. 4, p. 455, 2008.

[33] L. Harnefors, X. Wang, A. G. Yepes, and F. Blaabjerg, "Passivity-Based Stability Assessment of Grid-Connected VSCs—An Overview," *IEEE J. Emerg. Sel. Top. Power Electron.*, vol. 4, no. 1, pp. 116–125, Mar. 2016.

[34] K. Strunz, "Benchmark systems for network integration of renewable and distributed energy resources," in *Cigre Task Force C6.04.02*, July 2009.

[35] C. Yoon, X. Wang, F. M. F. Da Silva, C. L. Bak, and F. Blaabjerg, "Harmonic stability assessment for multi-paralleled, grid-connected inverters," in *2014 International Power Electronics and Application Conference and Exposition*, 2014, pp. 1098–1103.

[36] B. Gustavsen and A. Semlyen, "Enforcing Passivity for Admittance Matrices Approximated by Rational Functions," *IEEE Trans. Power Syst.*, vol. 16, no. 1, pp. 97-104, Feb. 2001.

[37] P. K. Goh, "Broadband Macromodeling Via A Fast Implementation Of Vector Fitting With Passivity Enforcement," Ph.D dissertation, University of Illinois at Urbana-Champaign, 2007.

[38] "PLECS, The Simulation Platform for Power Electronic Systems." [Online]. Available: https://www.plexim.com/plecs.

[39] M. K. Bakhshizadeh, J. Hjerrild, Ł. H. Kocewiak, F. Blaabjerg, C. L. Bak, X. Wang, F. M. F. da Silva, and B. Hesselbæk, "A Numerical Matrix-Based method in Harmonic Studies in Wind Power Plants," in *15th Wind Integration Workshop*, 2016, pp. 335–339.

[40] A. Rygg, M. Molinas, C. Zhang, and X. Cai, "A Modified Sequence-Domain Impedance Definition and Its Equivalence to the dq-Domain Impedance Definition for the Stability Analysis of AC Power Electronic Systems," *IEEE J. Emerg. Sel. Top. Power Electron.*, vol. 4, no. 4, pp. 1383–1396, Dec. 2016.

[41] B. Wen, D. Dong, D. Boroyevich, R. Burgos, P. Mattavelli, and Z. Shen, "Impedance-Based Analysis of Grid-Synchronization Stability for Three-Phase Paralleled Converters," *IEEE Trans. Power Electron.*, vol. 31, no. 1, pp. 26–38, Jan. 2016.

[42] K. R. Padiyar, *Analysis of Subsynchronous Resonance in Power Systems*. Springer Science & Business Media, 1999.

Mohammad Kazem Bakhshizadeh (S'16) received the B.S. and M.S. degrees in electrical engineering from the Amirkabir University of Technology, Tehran, Iran in 2008 and 2011, respectively. He is currently an industrial PhD student at Aalborg University, Aalborg, Denmark in collaboration with DONG Energy Wind Power, Fredericia, Denmark. In 2016, he was a visiting scholar at Imperial College London, London, U.K. His research interests include power quality, modeling and control of power converters, and grid converters for renewable energy systems.

Changwoo Yoon (S'08) received the B.S. and M.S. degrees from the Department of Control and Instrumentation Engineering, Seoul National University of Technology, Korea, in 2007 and 2009, respectively. He was an engineer at the Advance Drive Technology Co., Anyang, Korea from 2009 to 2013. He received his PhD in 2017 at the Department of Energy Technology (ET) at Aalborg University (AAU) in the field of small-scale power system stability. In 2015, he was a visiting scholar at University of Manitoba, Canada. His main research interests include power electronics for distributed generation, power quality and high power dc–dc converter for renewable energy.

Jesper Hjerrild was born in 1971. He holds an MSc and PhD degrees in electrical engineering from the Technical University of Denmark, Lyngby, in 1999 and 2002, respectively. Currently, he is employed with DONG Energy. His main technical interest is electrical power systems in general, involving a variety of technical disciplines including modeling of power system including wind power and power system control, stability and harmonics. Furthermore, he also works with designing of the wind farm.

Claus Leth Bak was born in Århus, Denmark, on April 13th, 1965. He received the B.Sc. with honors in Electrical Power Engineering in 1992 and the M.Sc. in Electrical Power Engineering at the Department of Energy Technology (ET) at Aalborg University (AAU) in 1994. After his studies he worked as a professional engineer with Electric Power Transmission and Substations with specializations within the area of Power System Protection at the NV Net Transmission Company. In 1999 he was employed as an Assistant Professor at ET-AAU, where he holds a Full Professor position today. He received the PhD degree in 2015 with the thesis "EHV/HV underground cables in the transmission system". He has supervised/co-supervised +35 PhD's and +50 MSc theses. His main Research areas include Corona Phenomena on Overhead Lines, Power System Modeling and Transient Simulations, Underground Cable transmission, Power System Harmonics, Power System Protection and HVDC-VSC Offshore Transmission Networks. He is the author/coauthor of app. 240 publications. He is a member of Cigré JWG C4-B4.38, Cigré SC C4 and SC B5 study committees' member and Danish Cigré National Committee. He is an IEEE senior member (M'1999, SM'2007). He received the DPSP 2014 best paper award and the PEDG 2016 best paper award. He serves as Head of the Energy Technology PhD program (+ 100 PhD's) and as Head of the Section of Electric Power Systems and High Voltage in AAU and is a member of the PhD board at the Faculty of Engineering and Science.

Łukasz Hubert Kocewiak (M'12, SM'16) holds BSc and MSc degrees in electrical engineering from Warsaw University of Technology as well as PhD degree from Aalborg University.
Currently he is with DONG Energy Wind Power and is working as a senior power system engineer on development of electrical infrastructure in large offshore wind power plants.
The main direction of his research is related to harmonics and nonlinear dynamics in power electronics and power systems especially focused on wind power generation units.
He is the author/co-author of more than 60 publications. He is a member of various working groups within Cigré, IEEE, IEC.

Frede Blaabjerg (S'86–M'88–SM'97–F'03) was with ABB-Scandia, Randers, Denmark, from 1987 to 1988. From 1988 to 1992, he got the PhD degree in Electrical Engineering at Aalborg University in 1995. He became an Assistant Professor in 1992, an Associate Professor in 1996, and a Full Professor of power electronics and drives in 1998. From 2017 he became a Villum Investigator.
His current research interests include power electronics and its applications such as in wind turbines, PV systems, reliability, harmonics and adjustable speed drives. He has published more than 450 journal papers in the fields of power electronics and its applications. He is the co-author of two monographs and editor of 6 books in power electronics and its applications.
He has received 18 IEEE Prize Paper Awards, the IEEE PELS Distinguished Service Award in 2009, the EPE-PEMC Council Award in 2010, the IEEE William E. Newell Power Electronics Award 2014 and the Villum Kann Rasmussen Research Award 2014. He was the Editor-in-Chief of the IEEE TRANSACTIONS ON POWER ELECTRONICS from 2006 to 2012. He has been Distinguished Lecturer for the IEEE Power Electronics Society from 2005 to 2007 and for the IEEE Industry Applications Society from 2010 to 2011 as well as 2017 to 2018.
He is nominated in 2014, 2015 and 2016 by Thomson Reuters to be between the most 250 cited researchers in Engineering in the world. In 2017 he became Honoris Causa at University Politehnica Timisoara (UPT), Romania.

Bo Hesselbæk received the M.Sc. degree in electrical engineering from Aalborg University, Aalborg, Denmark, and the MBA from the University of Southern Denmark, Odense, Denmark. The first years of his career, he was with the Danish Transmission System Operator both within transmission planning and operation. Since 2008, he has been with Vestas Wind Systems, Aarhus, Denmark, where he was Director of Vestas R&D America, until 2012, when he moved to DONG Energy Wind Power, Fredericia, Denmark, to head a department that designs the main electrical infrastructure of offshore wind farms. He holds multiple patents and publications